

Structural and Magnetic Studies on *Ni-Mn-Ga*-based Ferromagnetic Shape Memory Alloys

R.P. Mathur*, R.K. Singh, S. Ray#, M. Manivel Raja, P. Ghosal, and V. Chandrasekaran

Defence Metallurgical Research Laboratory, Hyderabad-500 058

#Indian Institute of Technology, Roorkee-247 667

*E-mail: mathur@dmrl.drdo.in

ABSTRACT

Quaternary $Ni_{50}Fe_xMn_{30-x}Ga_{20}$ ($x = 2.5, 5, \text{ and } 15$) and $Ni_{45}Fe_5Mn_{30}Ga_{20}$ alloys based on modification of ferromagnetic shape memory alloy ternary $Ni_{50}Mn_{30}Ga_{20}$ composition prepared by vacuum arc melting and subsequent heat-treatment were investigated to understand the effect of varying *Fe*-content in *Ni-Fe-Mn-Ga* alloys. With increasing *Fe*-content, saturation magnetisation and Curie temperature increased, however martensite transformation temperature did not show a systematic variation. The ^{57}Fe Mossbauer spectra showed three distinct sub-spectra depending upon the site occupancy by *Fe*-atoms. The results are explained with site selection by *Fe*-atom in parent $L2_1$ lattice.

Keywords: Ferromagnetic shape memory alloys, *Ni-Fe-Mn-Ga* alloys, Martensitic transformation, Mossbauer spectroscopy

1. INTRODUCTION

Ferromagnetic shape memory (FMSM) alloys are being increasingly used as active materials for smart devices as sensors, actuators and transducers. Their superiority over the conventional materials emerges from an optimal combination of work output and response time for the devices¹. Alloys based on Heusler Ni_2MnGa compositions have shown large magnetic field-induced strains of magnitude 6-10 per cent at room temperature²⁻⁵. The stoichiometric Ni_2MnGa alloy has an $L2_1$ structure (space group $Fm-3m$) and undergoes a magnetic transition at 376 K and structural martensite transformation at 202 K to a martensite structure. The martensite phase stability is reported to be affected by the number of average valance electrons per atom or the electron-to-atom ratio (*e/a* ratio). For *Ni-Fe-Mn-Ga* alloys, the *e/a* ratio is estimated using number of valance electrons as 10, 8, 7, 3 for each *Ni*, *Fe*, *Mn* and *Ga* atom, respectively⁶. Though *Ni* as well as *Mn*-rich off-stoichiometric ternary alloy compositions increase the martensite transformation temperatures^{7,8}, *Mn*-rich compositions with 5 or 7 layered modulated martensites structure and low detwining stresses are employed for FMSM applications^{4,9}. The *Mn*-substitution increases the martensite transformation temperatures; however, the Curie temperature is lowered⁸. Ternary $Ni_{50}Mn_{30}Ga_{20}$ (atom per cent) with an *e/a* ratio of 7.7 shows the maximum operating temperatures possible as martensite transformation temperatures approach Curie temperature¹⁰. The x-ray diffraction studies in $Ni_{1.95}Mn_{1.19}Ga_{0.86}$ have shown that excess *Mn* atoms occupy the *Ga*-sites of stoichiometric structure. Further alloy modifications within the vicinity of the *e/a*

ratio of 7.7 are investigated to improve properties without affecting the stability of martensite phase. Small additions of *Fe* are reported to lower the martensite transformation temperatures in *Ni-Mn-Ga* alloys¹¹. The relatively poor mechanical properties of the ternary *Ni-Mn-Ga* alloys are however improved by quaternary *Fe* addition¹².

The *Fe*-containing *Ni-Mn-Ga* quaternary alloys have been investigated with low *Fe*-additions¹¹ as well as with large additions as intermediate compositions between Ni_2MnGa and other Heusler compositions⁶. A single-phase structure with *Fe* within the solid solution has normally been reported in these studies. Mössbauer spectroscopy has been employed to investigate *Fe* atomic sites in Ni_2MnGa alloys using ^{57}Fe spectrum. The presence of *Fe* atoms at the *Ni*, *Mn* as well as *Ga* sites in ferromagnetic Ni_2MnGa with magnetic hyperfine field values of 8.6 T, 14.6 T and 14.5 T, respectively have been reported¹³. The Mössbauer spectrum for the $Ni_{40}Fe_{10}Mn_{30}Ga_{20}$ alloy has shown a low Mössbauer absorption of about 1.5 per cent and the presence of an additional paramagnetic doublet with the ferromagnetic spectrum of a sextet⁶. The paramagnetic state of a phase in structurally single-phase ferromagnetic alloys has not been investigated in detail. Other Heusler alloys containing *Fe* have similarly been investigated for *Fe*-site occupancy with paramagnetic spectra¹⁴⁻¹⁶. The present study was undertaken to investigate the effect of the substituting *Fe* atom, over a composition range as *Ni-Fe-Mn-Ga* quaternary alloys, on structural and magnetic transitions in these alloys and to correlate the atomic and magnetic structure of these alloys. Alloy compositions $Ni_{50}Fe_xMn_{30-x}Ga_{20}$ ($x = 2.5, 5 \text{ and } 15$ atom

per cent) were chosen in view of an earlier report⁶ that *Fe* atoms preferred manganese sites over nickel sites in the ordered structure. A $Ni_{45}Fe_5Mn_{30}Ga_{20}$ was also investigated identically to understand the effect of low *Fe* replacement for *Ni*. The observed structural and magnetic transitions in these quaternary alloys are reported correlating the results to the site selection by *Fe* atoms.

2. EXPERIMENTAL

Ni-Fe-Mn-Ga alloys (50 g each) were prepared using high purity elements (99.9 per cent purity) in an argon atmosphere by repeated arc melting to ensure homogenisation. The as-cast alloys were cut, sealed in evacuated quartz ampoules, and heat-treated at 1273 K for 72 h and 1073 K for 48 h in a vacuum furnace and then water quenched. The compositions of the alloys were determined from different places of the ingots by inductively-coupled plasma-optical emission spectroscopy (ICP-OES), energy dispersive x-ray spectroscopy (EDS) and electron probe micro-analysis (EPMA) techniques.

The heat-treated samples were cut, mounted, and polished. The samples were lightly etched with Kalling's reagent (50 cc *HCl* + 50 cc Methanol + 2-5 g $CuCl_2$) for microstructural examination. The microstructure of the alloys was observed using a Leo 440 scanning electron microscope. The x-ray diffraction patterns taken on a Philips PW1320 diffractometer with $Cu-K_{\alpha}$ radiation were used to investigate the crystal structure of the phases present at room temperature. The transformation temperatures were measured using a modulated differential scanning calorimeter (DSC) model Q100 (make TA instruments) under a constant heating/cooling rate of 20 K/min. A vibrating sample magnetometer (ADE make EV9 Model) was used for thermomagnetic measurements and magnetic measurements up to 20 kOe at room temperature. Thermomagnetic measurements were carried out at different temperatures with a low bias magnetic field of 500 Oe. The temperature of sample in heating cycle was raised in steps and stabilised magnetisation at a specific temperature was measured before going to the next step. The discreet changes in magnetisation have been related to the structural and magnetic transitions. Mössbauer spectra were recorded on a FAST Comtech spectrometer using ⁵⁷*Fe* gamma ray source. The spectrometer was calibrated with natural iron foils (25 μm thick) prior to data collection for the spectrum. In view of low Mössbauer fractions reported earlier for similar alloys^{6,17}, long time data acquisition was carried

out for counts exceeding 8×10^5 for each sample. The obtained spectra were analysed using PCMO5-II program using a line width of 0.35-0.40 mm/s. The isomer shifts are reported wrt natural iron.

2.1 Alloy Preparation

Alloys with nominal compositions (in atom per cent) $Ni_{50}Fe_xMn_{30-x}Ga_{20}$ ($x = 2.5, 5$ and 15) and $Ni_{45}Fe_5Mn_{30}Ga_{20}$ were prepared. Table 1 shows the alloy designations of the alloys prepared with their compositions as well as the average chemical compositions obtained through ICP-OES. Chemistry obtained through other techniques, viz. EPMA and EDS, was comparable to these values and it shows that the alloys to be close to their nominal compositions and thereby ensuring macro-homogeneity. The nomenclature 'A', 'B', 'C' and 'D' have been used to designate $Ni_{50}Fe_{2.5}Mn_{27.5}Ga_{20}$, $Ni_{50}Fe_5Mn_{25}Ga_{20}$, $Ni_{50}Fe_{15}Mn_{15}Ga_{20}$ and $Ni_{45}Fe_5Mn_{30}Ga_{20}$ alloys in subsequent text. Figure 1 shows the back-scattered electron images of the alloys. Alloys 'A', 'B' and 'D' have single-phase structures, whereas a two-phase structure was noticed for alloy 'C'. The average composition of the two phases in alloy 'C' analysed by EPMA was found to be $Ni_{49.09}Fe_{10.32}Mn_{19.74}Ga_{20.85}$ and $Ni_{43.45}Fe_{33.37}Mn_{13.40}Ga_{9.78}$ for the matrix and the embedded phase, respectively.

The x-ray diffractograms of the alloys obtained at a scan rate of $1^\circ(2\theta)/\text{min}$ are shown in Fig. 2(a). While the diffractograms for the alloys 'B' and 'D' could be indexed to tetragonal martensite phase similar to those obtained for *Ni-Mn-Ga* alloys¹⁸, those for the alloys 'A' and 'C' have shown additional peaks. The additional reflections for the alloy "A" (marked as • in Fig. 2(a)) disappear at higher *Fe* content. It may be noted that these reflection positions are nearer to super-lattice reflection positions of the parent austenite structure. In view of the two-phase structure of the alloy 'C', the diffractogram for the alloy 'C' has been indexed to a cubic austenite phase and un-indexed second phase (marked as * in Fig. 2(a)).

The (222) reflection of martensite phase splits in 2 or 3 peaks for chemically modulated super-period martensite 5M or 7M structures respectively. Additional peaks (marked by *) were noticed for single-phase alloys 'B'. Slower scans at $0.5^\circ(2\theta)/\text{min}$ around the (220) peak position were carried out and are presented in Fig. 2(b). The peak splitting is clear at slower scan for alloys 'A' and 'C' though reflections did not resolve clearly in case of alloy

Table 1. Nominal and analysed compositions of the arc-melted *Ni-Fe-Mn-Ga* alloys

Alloy designation	Nominal composition								Analysed bulk chemistry			
	Atomic per cent				Wt. per cent				Wt. per cent			
	<i>Ni</i>	<i>Fe</i>	<i>Mn</i>	<i>Ga</i>	<i>Ni</i>	<i>Fe</i>	<i>Mn</i>	<i>Ga</i>	<i>Ni</i>	<i>Fe</i>	<i>Mn</i>	<i>Ga</i> (by difference)
A	50	2.5	27.5	20	49.08	2.33	25.27	23.32	50.0 ± 0.60	2.78 ± 0.10	28.20 ± 0.20	19.02
B	50	5	25	20	49.06	4.67	22.96	23.31	49.5 ± 0.60	5.18 ± 0.10	25.90 ± 0.20	19.92
C	50	15	15	20	48.98	13.98	13.76	23.28	49.0 ± 0.60	13.9 ± 0.25	18.0 ± 0.20	19.1
D	45	5	30	20	44.29	4.68	27.64	23.39	44.5 ± 0.60	6.25 ± 0.20	29.05 ± 0.20	20.2

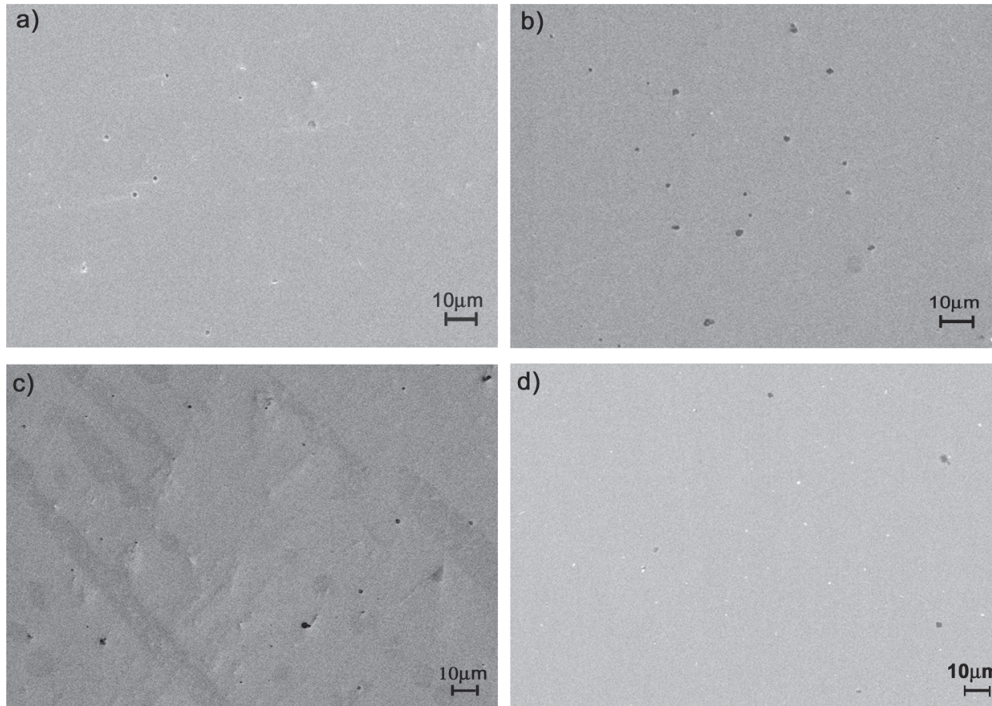


Figure 1. Backscattered electron image: (a) of alloy ‘A’ ($Ni_{50}Fe_{2.5}Mn_{27.5}Ga_{20}$), (b) of alloy ‘B’ ($Ni_{50}Fe_5Mn_{25}Ga_{20}$), (c) of alloy C ($Ni_{50}Fe_{15}Mn_{15}Ga_{20}$) and (d) of alloy D ($Ni_{45}Fe_5Mn_{30}Ga_{20}$).

‘B’ to confirm the modulated structure. The additional peak positions in alloy ‘B’ matches with that of the secondary phase in case of alloy ‘C’. Modulated martensite structure in *Ni-Mn-Ga* systems forms due to thermo-mechanical treatments in suitable compositions. Overlapping reflections in diffractograms either indicate a transitional stage from a non-modulated to modulated structure or the formation of very fine secondary phase unresolved in microstructure. Chemical composition variations via spinodal reactions

during $B2' \rightarrow L2_1$ ordering has also been reported in the *Ni-Mn-Ga* alloys¹⁹ and may also cause the splitting of reflections. No sinusoidal compositional variations were however seen during compositional analysis of the alloys.

2.2 Thermal Analysis

The DSC thermograms obtained for the alloys investigated shows the exotherms during cooling and endotherms during heating cycles (Fig. 3). These events

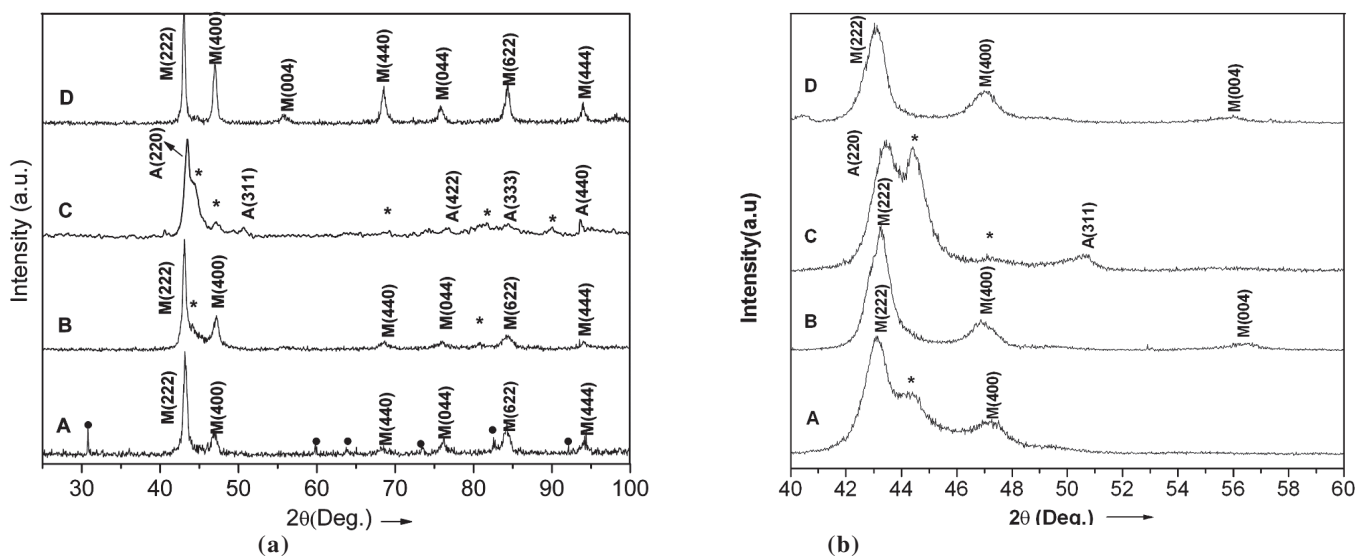


Figure 2. X-ray diffractograms ($Cu K_{\alpha}$) taken: (a) at a scan rate of $1^{\circ} (2\theta)/min$, and (b) at a scan rate of $0.5^{\circ} (2\theta)/min$ for the alloys ‘A’, ‘B’, ‘C’ and ‘D’. The phases identified (M-martensite and A-austenite) are marked with their reflections. The secondary phase in alloy ‘D’ is marked with *. The ● for alloy ‘A’ shows the reflections disappearing on random placement of Fe in other alloys.

are attributed to structural martensite transformation and reverse transformation to austenite, respectively. The observed transformation temperatures (martensite start T_{ms} and finish T_{mf} and austenite start T_{as} and finish T_{af} temperatures) as well as the transformation enthalpies from the thermograms are shown in Table 2. Measurements from the previous report⁶, wherein the *Fe*-substitution was intended for *Ni* have been included for comparison. The martensite transformation temperatures increase from alloy 'A' to alloy 'B', *i.e.* from 2.5 per cent *Fe* to 5 per

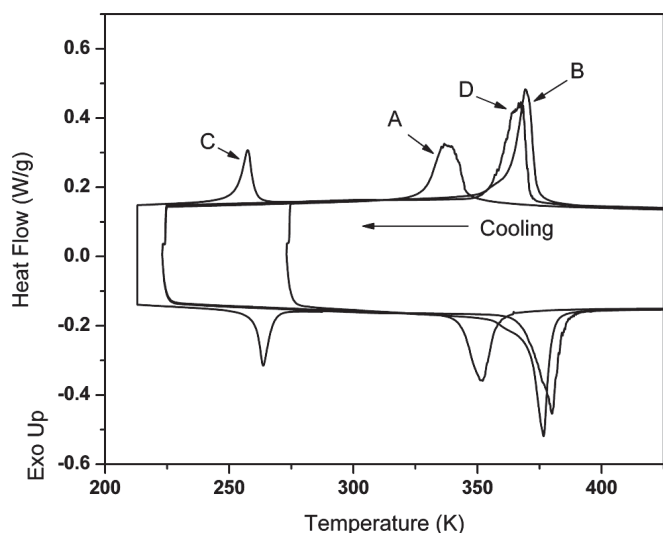


Figure 3. DSC thermograms for the alloys 'A', 'B', 'C', and 'D'.

cent *Fe* in line with increasing *e/a* ratio. These values are lower for alloy 'C'. In addition, alloy 'C' showed a transformation enthalpy value of 2.67 J/g, which is much lower than that of the other alloys. In view of the two-phase structure of the alloy (Fig. 1(c)), this value appears to be lowered due to contributions of transformation enthalpy from only one of the two phases. Extended thermal scans up to the instrument limits (673 K) were carried out and did not however reveal the transformation peaks for the second phase in the case of alloy 'C'.

2.3 Magnetic and Thermomagnetic Measurements

Fig. 4(a) shows the room temperature magnetisation (*M-H*) curves of the alloys. The alloy "B" showed a two-stage behaviour in the middle segments in both first and third quadrant of the curve. The alloy 'C' with a two phase microstructure showed a hysteresis, but magnetisation curve did not show two-stage behaviour. The saturation magnetisation (M_s) values obtained were 30.66 emu/g, 33.83 emu/g, 53.68 emu/g and 22.93 emu/g for alloys 'A', 'B', 'C' and 'D', respectively. The room temperature measurements for the alloys are nearer to their Curie temperature. Considering the mixed-phase structure and thermal disturbances around Curie temperatures, low-temperature measurements below the martensite transformation temperatures were taken at 173K. The results of such measurements are presented in Fig. 4(b). All the curves at low temperatures showed a well defined hysteresis commensurate with the anisotropic martensite phase. The saturation magnetisation values at 173K for alloys 'A', 'B', 'C' and 'D' are 47.76 emu/g, 37.18 emu/g, 63.92 emu/g and 39.29 emu/g, respectively. The alloys 'B' and 'D' show comparable magnetisation, with alloy 'B' showing a lower magnetisation rate and thus higher anisotropy.

The thermomagnetic *M-T* measurements for the alloys are shown in Fig. 5. The alloys 'A' and 'D' show a fall in magnetisation to zero *i.e.* to a paramagnetic state. Alloy 'B' shows a rise in magnetisation with increasing temperature prior to a fall due to paramagnetic (Curie) transitions. The saturation magnetisation of martensite phase is normally higher than that of the corresponding austenite phase. However, these phases are more anisotropic than their cubic counterparts and the rise in specific magnetisation at low biasing field with increasing temperature is attributed to the martensite-to-austenite transformation. The alloy 'C' showed three transitions; a rise in magnetisation around 250-275 K, an intermediate fall in magnetisation around 275-325 K and final transition to a paramagnetic state 375-440 K. In view of the two phase structure these stages show two martensite to austenite transformations, Curie transition of the austenite phase and the Curie transformation of the second phase, respectively. The martensite transformation

Table 2. Transformation temperatures and enthalpies of transformation for the alloys investigated

Alloy Designation	<i>e/a</i> ratio [#]	Martensite transformation			Austenite transformation		
		Transformation temperature (K)		Enthalpy (J/g)	Transformation temperature (K)		Enthalpy (J/g)
		Start (T_{ms})	Finish (T_{mf})	$\Delta H_{A \rightarrow M}$	Start (T_{as})	Finish (T_{af})	$\Delta H_{M \rightarrow A}$
'A'	7.625	345	328	6.24	342	358	5.99
'B'	7.750	374	360	8.69	364	382	8.80
'C'	7.850	261	252	2.57	259	269	2.67
'D'	7.600	371	356	8.77	367	385	8.46
$Ni_{40}Fe_{10}Mn_{30}Ga_{20}$ [@]	7.500	206	183	-	191	224	-

[#] (10*at%Ni + 8*at%Fe + 7*at%Mn + 3*at%Ga)/100, [@] Cited for comparison⁶

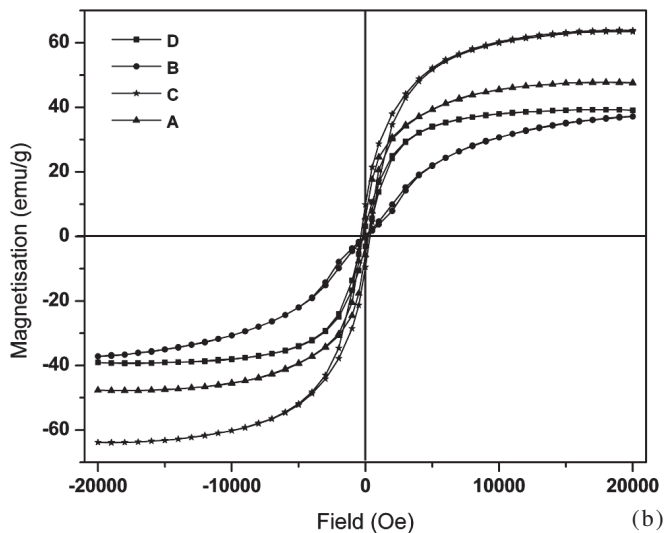
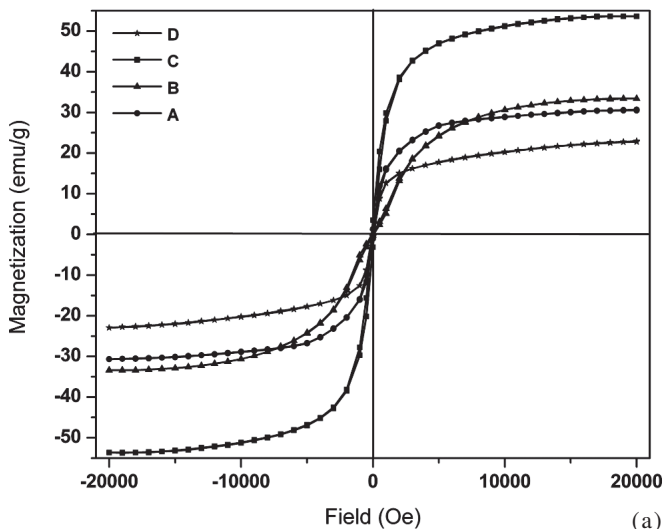


Figure 4. The magnetisation curves of the alloys ‘A’, ‘B’, ‘C’ and ‘D’ : (a) at room temperature, and (b) at 173 K.

temperatures obtained in our thermo-magnetic measurements for the alloys ‘B’ and ‘C’ are comparable to those observed through DSC.

2.4 Mossbauer Experiments

Figure 6 shows the room temperature spectra of the alloys investigated. The spectra obtained with counts exceeding 8×10^5 shows the Mössbauer absorption fraction limited to about 1.5 per cent. Similar Mössbauer fractions have been reported earlier for *Ni-Mn-Ga* alloys⁶. The low fractions have contributed to a higher scatter to the obtained spectra, specially at the lowest *Fe* content of 2.5 per cent, though the scatter is lowered at higher *Fe*. As the sampling data space is reasonably large, the obtained scatter is not attributable to the instrument, data collection, but to a lower recoil-free fraction of the incident photons. The recoil-free fraction of the absorption is a factor of various material-dependent parameters, such as the lattice vibrations, i.e., phonons, Debye temperature¹⁷. The *Ni-Mn-Ga* alloys

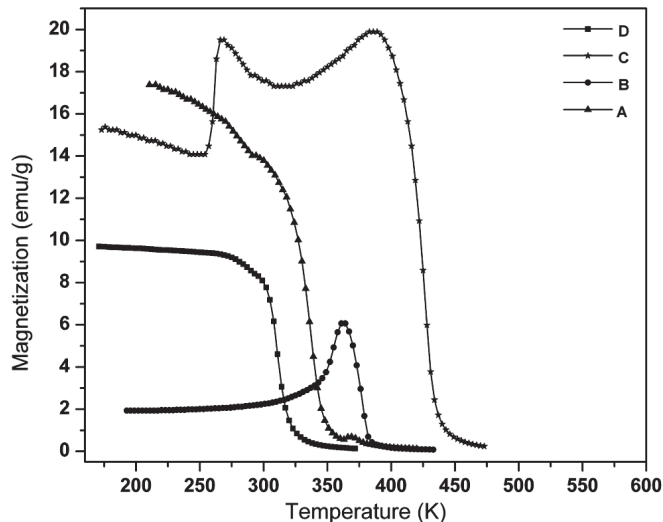


Figure 5. Thermomagnetic measurements for the alloys ‘A’, ‘B’, ‘C’ and ‘D’.

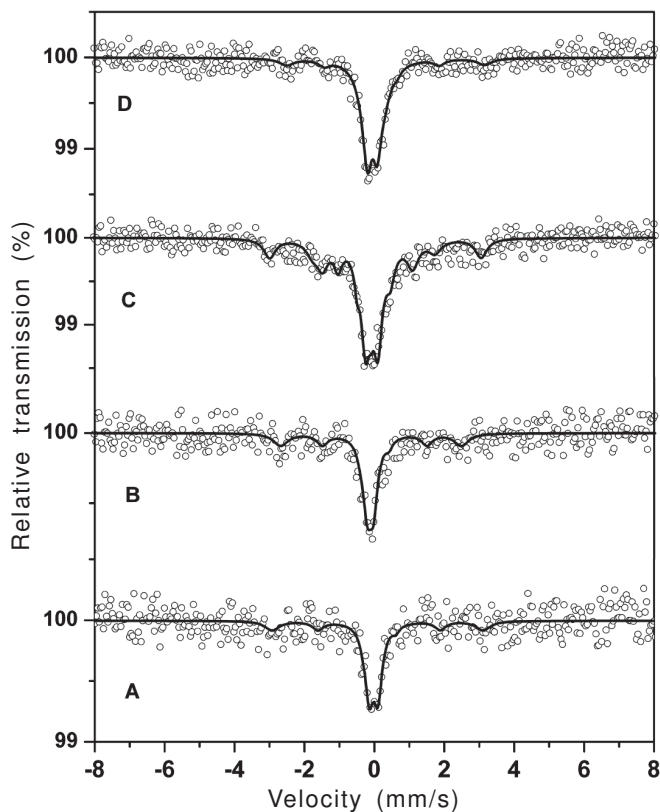


Figure 6. Mossbauer spectra of the alloys ‘A’, ‘B’, ‘C’ and ‘D’ taken at room temperature. The solid line indicates the fitting curve with parameters shown in Table 3.

show Debye temperatures of the order of 383-400 K, almost independent of compositions²⁰. These alloys have a singular lattice dynamic behaviour showing softening of the TA_2 branch phonons around $\xi = (1/3, 1/3.0)$ on cooling, and thereby, displaying a phenomenon commonly referred as pre-martensite phenomenon²¹. It appears that low recoil-free fractions are material characteristics and could have been overcome using enriched *Fe*. Natural *Fe* was used while

preparing our alloys; however, the obtained absorption spectra could be reasonably analysed using least square fit to understand the underlying pattern for the alloys. The spectra could be de-convoluted to a sub-spectrum of a doublet and a sextet in case of alloys 'A' and 'B', and into a doublet and two sextets in case of alloys 'C' and 'D'. The calculated fitting curves are also shown in Fig. 6. The Mössbauer parameters derived from the observations and fitting parameters are compiled in Table 3. Alloy 'A' shows the presence of a ferromagnetic sextet and a paramagnetic doublet. The paramagnetic contribution of the spectrum goes down on increasing the *Fe* content to 5 per cent (alloy 'B'). The spectrum for a second ferromagnetic sextet is seen either at higher *Fe* content of 15 at per cent for both two phase alloy 'C' as well as the single phase alloy 'D'. For a comparable substitution of 5 per cent *Fe*, alloy 'D' with *Fe* substituting for *Ni* showed larger fraction of paramagnetic fraction.

3. RESULTS AND DISCUSSION

The stoichiometric alloys Ni_2MnGa has an $L2_1$ structure (Fm $\bar{3}m$) at higher temperature with unit cell showing four formulae unit with 8 *Ni*-atoms at the centres of the quartets and *Mn* and *Ga*-atoms arranged alternating at the edges. Martensite structures have been derived from the $L2_1$ structure in tetragonal or orthorhombic systems for various modulated/non-modulated martensites²². X-ray diffraction patterns for *Mn*-rich $Ni_{1.95}Mn_{1.19}Ga_{0.86}$ super-period 5M martensite phase have been fitted using Rietveld refinement²³. The similar atomic scattering factors for *Ni* and *Mn* atoms did not allow the distinction between *Ni* and *Mn* atoms and fitting was reported using $Ni_2Mn_{1.15}Ga_{0.85}$ composition on monoclinic I2/m basis with *Ni*-atoms at 4h, *Mn*-atoms at 2a and *Ga*-atoms at 2d sites and excess *Mn*-atoms at 2d *Ga*-sites.

By analogy, *Fe* atoms substituting for *Mn* in the

$Ni_{50}Fe_xMn_{30-x}Ga_{20}$ alloys for $x \geq 5$ should place themselves at *Mn*- or *Ga*-sites. Alloy 'A' and 'B' have shown single phase structures (Fig. 1) and the x-ray diffractograms (Fig. 2) for these alloys are indexed to tetragonal martensite structure. The extra reflections in diffractogram for the alloy "A" with 2.5 per cent *Fe* however are not reported in case of studies on ternary $Ni_{50}Mn_{30}Ga_{20}$ alloys. Their presence and subsequent annulment at 5 per cent *Fe* suggest a more random presence of *Fe* atoms at different atomic sites at higher *Fe* concentrations. The Mössbauer spectra for these alloys have shown two sub-spectra for the presence of *Fe* in ferromagnetic as well as paramagnetic environments indicating the two coexisting magnetically different but structurally similar phase structures in the alloys. Chemical ordering in Heusler *Ni-Mn-Ga* alloys is reported to cause spinodal type compositional variations and could have resulted in phase separations. The *Fe* sub-spectra in some of these alloys in three different sub-spectra confirm the position of *Fe* atoms in three magnetically different sites, viz., *Ni*, *Mn* and *Ga* sites in Ni_2MnGa alloys. With the Heusler alloy formula X_2YZ , these sites are indicated as X, Y or Z sites for the *Ni*, *Mn* or *Ga* sites, respectively. The hyperfine fields of the sextets fall in two broad categories; with higher values in the range 17-19T and with lower values of 8.2 and 9.5 T. The higher set of values compared to 33.0 T (2.2 μ_B per *Fe* atom) for pure *Fe* signifies the presence of *Fe* at atomic sites in predominantly ferromagnetic environment²⁴. The Y-sites or *Mn* sites, being the primary contributor to magnetic moment in Ni_2MnGa alloys, the *Fe* atoms contributing to higher hyperfine field values of *Fe* indicate their occupation of the Y or the manganese sites. The intensity of *Fe* spectrum in paramagnetic phase has gone down from 82 per cent to 54 per cent with increase of *Fe* from 2.5 per cent to 5 per cent. The *Fe* in paramagnetic state at room temperature shows the Curie temperature of this constituent to be lower than room temperature.

Table 3. Mossbauer parameters hyperfine magnetic field (H_{hf}), quadrupole splitting (QS), isomer shift (IS) and relative intensities for the ^{57}Fe Mössbauer spectra in *Ni-Fe-Mn-Ga* alloys

Alloy Designation	Hyperfine parameters					Remarks
	Sub-spectrum	H_{hf}	QS	IS	Intensity %	
		Tesla (μ_B) $\pm 0.2T$	(mm/s) ± 0.05 mm/s	(mm/s) ± 0.002 mm/s		
A	Sextet	18.5(1.23)	0.05	0.110	18	Y-site (Mn-site)
	Doublet	--	0.26	-0.028	82	Z-site (Ga-site)
B	Sextet	17.0(1.13)	0.10	-0.047	46	Y-site (Mn-site)
	Doublet	--	0.18	-0.033	54	Z-site (Ga-site)
C	Sextet	8.2(0.55)	0.13	-0.237	13	X-site (Ni-site)
	Sextet	19.0(1.26)	0.07	-0.016	38	Y-site (Mn-site)
	Doublet	--	0.35	-0.077	50	Z-site (Ga-site)
D	Sextet	9.5(0.63)	0.12	0.140	13	X-site (Ni-site)
	Sextet	17.5(1.16)	0.11	-0.008	17	Y-site (Mn-site)
	Doublet	--	0.26	-0.050	70	Z-site (Ga-site)
$Ni_{40}Fe_{10}Mn_{30}Ga_{20}$ [@]	Sextet	29.3(1.95)	#	#	92	Y-site (Mn-site)
	Doublet	#	#	#	8	Z-site (Ga-site)

@ Cited in literature⁶ for comparison, # denotes the values not reported.

Gallium addition is reported to lower Curie temperature in ternary *Ni-Mn-Ga* alloys¹⁸. Placement of *Fe* at *Ga* site is consistent with this observation as well as with the reports of excess *Mn* in *Mn*-rich ternary alloys placed at *Ga* sites²³. The fall in paramagnetic contribution signifies that while majority of *Fe* at 2.5 per cent *Fe* levels is placed at *Ga*-sites, further placement of *Fe* is at different sites. Values of hyperfine field for ⁵⁷*Fe* at the *Ni*, *Mn* and *Ga* sites in ferromagnetic *Ni₂MnGa* structure at room temperature are reported as 8.6, 14.6 and 14.5 T respectively¹³. The presence of *Fe* giving spectra with hyperfine field values 18.5 and 17.0 T shows the placement of the contributing *Fe* atoms at *Mn* sites in case of alloys 'A' and 'B'.

The x-ray diffraction pattern for alloy 'B' with a single-phase structure was indexed to a single-phase martensite except for un-indexed peaks marked with * in Fig. 2(a). As pointed out earlier, these peaks can occur due to various reasons such as a chemical modulation (modulated super period 5M martensite), spinodal type phase separation or a different chemical species. The possibility of a different phase structures should be considered in conformity with peak position for the alloy 'C'. The alloy 'C' had shown the presence of a second phase with a matrix containing 10 per cent *Fe*. With about 10 per cent *Fe* soluble in the *Ni₅₀Mn₃₀Ga₂₀* in the matrix phase, single-phase structure of the alloy 'B' appears to be in order. The heat treatment imparted in this study is water quench following homogenisation at higher temperature. In absence of the detailed phase diagrams for the alloy system, the possibility of the alloy passing through a two phase field region in the intermediate temperature range can not be completely ruled out. The Mössbauer spectrum for the alloy 'B' however could not be fitted into 3 sub-spectra patterns. The extra x-ray diffractogram reflection between M(222) and M(400), if assigned to a second phase, should have given a different Mössbauer spectrum sextet in a more sensitive technique to *Fe* atoms. In the absence of evidence of *Fe* in a different chemical environment, the possibility of a second phase is ruled out. The satellite peak to (220) peak reflection in case of alloy 'B' therefore suggests a modulated martensite phase in its formative stages, resulting in overlapped peaks in the diffractograms. The broadening of other martensite reflections compared to that for alloy "A" has to be viewed in the context.

Alloy 'C' with 15 per cent *Fe* replacing *Mn* in the base composition is a two-phase alloy (Fig. 1(c)). The analysed phase compositions revealed the matrix phase to be *Ni₅₀Mn₃₀Ga₂₀* type with about 10 per cent *Fe* replacing the *Mn*. *Fe* additions beyond the solubility limit formed a second phase rich in *Ni* and *Fe*. Martensite transformations in DSC and M-T curves and first Curie transition in M-T curve can be assigned to the matrix phase based on its composition.

The second Curie transition at higher temperature is assigned to the second phase. Transformation

temperatures for high temperature shape memory *Ni-Mn-Ga* Heusler alloys are limited to about 673 K. With the chemical composition of the second phase off Heusler compositions, the second phase in alloy 'C' did not undergo any martensite transformation. The Curie transformation temperatures of the order of those obtained for this phase are normal in binary *Ni-Fe* system²⁵. The Mössbauer spectrum for the alloy could be de-convoluted to pattern of a paramagnetic phase and two ferromagnetic sextets with hyperfine fields (H_{hf}) of 8.2 T and 19.0 T. The sextet with H_{hf} of 19.0 T is attributable to *Fe* placed at *Mn* sites, the sextet with H_{hf} of 8.2 T signifies a placement at *Ni* sites. With two ferromagnetic phases in the alloy "C", two sextet patterns showed the *Fe* in two different chemical environments. Possibility of *Fe* placed additionally at *Ni* sites in the matrix phase and thus contributing to the second sextets cannot be ruled out in view of the similarity in the hyperfine field of *Fe* at *Ni* sites in the Heusler structure¹³. The *Fe* atoms for the second ferromagnetic sextet could have resulted with *Fe* placed at *Ni* sites in either of the phases for the alloy 'C'.

Alloy 'D' with 5 per cent *Fe* replacing *Ni* in formulae *Ni₅₀Mn₃₀Ga₂₀* has shown a single-phase structure with diffractogram showing tetragonal martensite structure. The Mössbauer pattern in this case consisted of a doublet and two sextets showing the presence of *Fe* in three different sites, viz., *Ni*, *Mn* and *Ga* sites. Our Mössbauer results therefore indicate the presence of *Fe* atoms at the atomic positions in order of filling preference of *Ga*, *Mn* and *Ni*. With the investigated compositions in *Ga* lean side of the stoichiometry, *Fe* placement at *Ga* sites preferentially appears to be in order.

The presence of sextet in alloy 'D' corresponding to *Fe* placement at *Ni* sites may similarly be related to a *Ni*-lean composition. It may be noted that previous report⁶ for *Ni₄₀Fe₁₀Mn₃₀Ga₂₀* had shown one sextet for *Fe* placed at *Mn*-sites in an alloy much leaner in *Ni*. It may however be noted that the heat treatment imparted in the earlier study was for a higher temperature, lower duration treatment as compared to that in the present study. Quenching from higher temperature has been reported to lower intermediate martensite transformation temperatures by affecting the L2₁ order degree²⁶. A lower temperature heat-treatment around the ordering temperature could have helped in forming the ordered structure with *Fe* placed at different sites. The ferromagnetic sub-spectrum corresponding to *Fe* placement at *Mn* sites in an *Ni*-lean compositions however cannot be explained only by the constitutional vacancies as our compositions are *Mn*-rich compositions. It may be pointed out here that the atomic sizes of constituent atoms in *Ni-Mn-Ga* alloys decrease from *Ga* to *Mn* to *Ni* (1.81 Å, 1.79 Å and 1.62 Å for atomic radii and 1.17 Å, 1.17 Å and 1.15 Å for covalent radii, respectively). *Fe* atom placement therefore follows the order of atomic sizes from larger space to smaller space.

An increase in transformation temperatures is noticed from *Fe* levels of 2.5 at per cent to 5 at per cent, however the transformation temperature has fallen drastically at higher *Fe* levels of 15 per cent. Ternary *Ni-Mn-Ga* alloys with *e/a* ratio of 7.7 are reported to possess a modulated martensite structure at room temperatures²⁷ and the transformation temperatures were expected to rise with an increase in *e/a* ratio, i.e., the *Fe* content. In view of the two-phase structure, meaningful correlations are not possible for the alloy 'C' with the average *e/a* ratio. The average *e/a* ratio for the matrix phase analysed to be $Ni_{49.09}Fe_{10.32}Mn_{19.74}Ga_{20.85}$ works out to be 7.77 and should have shown moderate transformation temperatures. It may be noted that a higher *e/a* ratio indicates that an increased density of state at Brillouin zone imparting increased martensite stability. The alloy 'C' has shown the presence of *Fe* in three different sites in the Mössbauer spectrum with one ferromagnetic sextet assignable to both the matrix and the secondary phase. The actual density of states in such a case would be completely different in the matrix phase than any *e/a* ratio assignment. The lower martensite stability in case of high *e/a* ratio alloy 'C' is indicative of a different chemical environment prevailing in the alloy than the low *Fe* alloys.

Alloys 'B' and 'D' with 5 per cent *Fe* substituting for *Mn* and *Ni*, respectively in formulae have shown comparable martensite transformation temperatures within ~3K. Based on a higher *e/a* ratio, the expected martensite transformation temperatures for the alloy 'B' were expected to be higher than those observed. Placement of *Fe* at *Ni*-sites for alloy 'D' as compared to that on *Mn*-sites for alloy 'B' shows different chemical environments modifying the density of state in a different fashion for lowering of the transformation temperatures.

Increase in saturation magnetisation at room temperature is evident with increasing *Fe*, i.e., going from alloy "A" to 'C'. Both the alloys 'B' and 'D' contain 5 atom per cent *Fe*, however the saturation magnetisation of alloy B is higher than that for the alloy 'D' and supports the earlier report⁶ that the magnetisation is higher with *Fe* atom at *Mn* site. These values are however lower than the reported values of 64 emu/g for stoichiometric Ni_2MnGa alloy⁸ and ~50 emu/g for ternary $Ni_{50}Mn_{30}Ga_{20}$ alloy²⁸. The low temperature measurements measuring magnetisation with martensite phase showed the alloy "B" with lowest magnetisation. Ternary Ni_2MnGa alloys show a magnetisation of 4.13 μ_B per *Mn* atom with only 0.30 μ_B contribution per *Ni* atom and a negligible (-0.05 μ_B) contribution from *Ga* atoms²⁹. A fall in magnetisation in ternary alloys is reported on either side of the stoichiometric composition due to dilution effect on one side and change of coupling from ferromagnetic to anti-ferromagnetic on the other side. The structure of the alloys revealed through x-ray diffraction has suggested a transition in *Fe* sites after the alloy "A". As *Fe*-atoms are present at different sites, a combination

of the dilution and modified inter-atomic coupling behaviour will change the magnetisation values in the manner observed. The magnetic measurements therefore were consistent with *Fe* atoms at magnetically different sites. Small amounts of hysteresis present in the alloys suggest the presence of anisotropic phase, viz., the martensite phase. As the alloys have displayed the anisotropic martensite structure, observed non-zero values of quadrupole splitting in all the sub-spectra confirms such anisotropy for *Fe* sites. With four chemical species present in the alloys, the *Fe* nuclei at different positions are in different chemical environments reflected in the isomer shift values.

4. CONCLUSIONS

- (i) $Ni_{50}Fe_xMn_{30-x}Ga_{20}$ ($x=2.5, 5$ and 15) and $Ni_{45}Fe_5Mn_{30}Ga_{20}$ alloys have been systematically investigated to understand the effect of *Fe* additions on structural and magnetic transitions in *Ni-Fe-Mn-Ga* alloys.
- (ii) Single-phase structure is revealed for the alloys up to 5 per cent *Fe*. The alloy with 15 per cent *Fe* however shows a two-phase structure showing a limited solubility of *Fe* in the $L2_1$ structure. The alloys showed a martensite/ austenite structure at room temperature depending upon the transformation temperatures. The additional x-ray reflections in low *Fe* containing alloy disappeared at higher *Fe* content indicative of a different site occupation of *Fe* atoms.
- (iii) The ^{57}Fe -Mössbauer spectra confirmed the presence of *Fe* atoms in three distinct sub-spectra. The obtained spectra can be explained with *Fe*-atoms following an occupation sequence $Ga \rightarrow Mn \rightarrow Ni$ at the constitutional vacancy or a preference to specific sites due to atomic size considerations.
- (iv) The Curie temperature of quaternary *Ni-Fe-Mn-Ga* increased with increasing *Fe* content; however martensite transformation temperature did not show a systematic variation. The saturation magnetisation increased with increasing *Fe* content at room temperature with low temperature saturation magnetisation not following the room temperature behaviour. The martensite transition temperatures do not strictly follow an electron-to-atom ratio dependence. These results could be explained with *Fe* atom placement in sites with different chemical environments at different *Fe* content.

ACKNOWLEDGEMENTS

The authors are thankful to Defence Research & Development Organisation (DRDO) for the financial support through a project. Authors express their thanks to Dr G Malakondaih, Distinguished Scientist, Director, Defence Metallurgical Research Laboratory, Hyderabad, for his constant encouragement and permission to publish these results. Thanks are also due to Prof L Manosa for his critical comments on our thermomagnetic data.

REFERENCES

- Wilson, S.A.; Jourdain, R.P.J.; Zhang, Q.; Dorey, R.A.; Bowen, C.R.; Willander, M. & Wahab, Q.U. New materials for micro-scale sensors and actuators: An engineering review. *Mater. Sci. & Engg.*, 2007, **56**, 1.
- Ullakko; Huang, K.J.; Kantner, C.; Handley, R.C.O. & Kokorin, V.V. Large magnetic field-induced strains in *Ni₂MnGa* single crystals. *Appl. Phys. Lett.*, 1996, **69**, 1966.
- Kakeshita, T. & Ullakko, K. Giant magnetostriction in ferromagnetic shape-memory alloys. *MRS Bulletin*, 2002, **105**, 105.
- Soderberg, O.; Sozinov, Y.Ge.A.; Hannula, S.P. & Lindros, V.K. Recent breakthrough development of the magnetic shape memory effect in *Ni-Mn-Ga* alloys. *Smart Mater. Struct.*, 2005, **14**, 223.
- Wuttig, M.; Liu, L.; Tsichiya, K. & James, R.D. Occurrence of ferromagnetic shape memory alloys. *J. Appl. Phys.*, 2000, **87**, 4707.
- Mathur, R.P.; Singh, R.K.; Chandrasekaran, V.; Ray, S. & Ghosal, P. Structural and magnetic transitions in *Fe*-, *Co*- and *Al*-substituted *Ni-Mn-Ga* ferromagnetic shape memory alloys. *Metal Mater. Trans. A*, 2007, **38**, 2076.
- Entel, P.; Bucholnikov, V.D.; Khovailo, V.V.; Zayak, A.T.; Adeagbo, W.A.; Gruner, M.E.; Harper, H.C. & Wasserman, E.F. Modelling the phase diagram of magnetic shape memory Heusler alloys. *J. Phys. D: Appl. Phys.*, 2006, **39**, 865.
- Jin, X.; Marioni, M.; Bono, D.; Allen, S.M. & O'Handley, R.C. Empirical mapping of *Ni-Mn-Ga* properties with composition and valence electron concentration. *J. Appl. Phys.*, 2002, **91**, 8222.
- Jiang, C.; Muhammad, Y.; Deng, L.; Wu, W. & Xu, H. Composition dependence on the martensite structures of *Mn*-rich *NiMnGa* alloys. *Acta Materialia*, 2004, **52**, 2779.
- Chernenko, V.A. Compositional instability of beta phase in *NiMnGa* alloys. *Scripta Materialia*, 1999, **40**(5), 523-27.
- Khovailo, V.V.; Abe, T.; Koledov, V.V.; Matsumoto, M.; Nakamura, H.; Note, R.; Ohtsuka, M.; Shavrov, V.G. & Takagi, T. Influence of *Fe* and *Co* on phase transformations in *Ni-Mn-Ga* alloys. *Mater. Trans.-JIM*, 2003, **44**, 2509.
- Xu, H.B.; Li, Y. & Jiang, C.B. *Ni-Mn-Ga* high-temperature shape memory alloys. *Mater. Sci. Engg. A*, 2006, **438-40**, 1065.
- Mitros, C.; Yehia, S.; Kumar, S.; Jha, S.; DeMarco, M.; Mitchell, D.; Julian, G.M. & Dunlap, R.A. Hyperfine magnetic field measurements in Heusler alloys *Ni₂MnGa*, *Pd₂MnSn*, and *Ru₂FeSn*. *Hyperfine Interactions*, 1987, **34**, 419.
- Gutierrez, P.; Lazpita, J.; Garitaonandia, J.S.; Chernenko, V.A. & Kanomata, K. Mossbauer study of the martensitic transformation in a *Ni-Fe-Ga* shape memory alloy. *Hyperfine Interactions*, 2006, **168**, 1207.
- Leiper, W.; White, C.G.; Judah, J. & Blaauw, C. Hyperfine fields *Fe* impurity in the *Co*-based Heusler alloy *Co₂(Ti, Hf, V)Al*. *J. Magntsm. Mag. Mater.*, 1980, **15-18**, 639-40.
- Leiper, W.; Mackay, G.R. & Blaauw, C. *J. Appl. Phys.*, 1978, **49**, 1552 -.
- Wertheim, G.K. Mössbauer effect : Principles and applications. Academic Press, 1971.
- Singh, R.K.; Shamsuddin, M.; Gopalan, R.; Mathur, R.P. & Chandrasekaran, V. *Mater. Sci. Engg. A*, 2008, **476**, 195.
- Overholser, R.W.; Wuttig, M. & Neumann, D.A. Chemical ordering in *Ni-Mn-Ga* Heusler alloys. *Scripta Materialia*, 1999, **40**, 1095.
- Matsumoto, M.; Ebisuya, M.; Kanomata, T.; Note, R.; Yoshida, H. & Kaneko, T. Magnetic properties of Heusler type *Ni_{2+x}Mn_{1-x}Ga*. *J. Magntsm. Mag. Mater.*, 2002, **239**, 521.
- Manosa, L. & Planes, A. Phonon softening in *Ni-Mn-Ga* alloys. *Physics Review. B*, 2001, **64**, 024305.
- Brown, P.J.; Crangle, J.; Kanomata, T.; Matsumoto, M.; Neumann, K.U.; Ouladdiaf, B. & Ziebeck, K.R.A. The crystal structure and phase transitions of the magnetic shape memory compound *Ni₂MnGa*. *J. Phys. Condens. Matter*, 2002, **14**, 10159.
- Righi, L.; Albertini, F.; Pareti, L.; Paoluzi, A. & Calestani, G. Commensurate and incommensurate "5M" modulated crystal structures in *Ni-Mn-Ga* martensitic phases. *Acta Materialia*, 2007, **55**, 5237.
- Hanna, S.S.; Heberie, J.; Littlejohn, C.; Perlow, G.J.; Preston, R.S. & Vincent, D.H. Mössbauer studies in natural iron. *Phy. Rev. Letts.*, 1960, **4**, 177.
- Lacheisserie, E.T. & Gignoux, D. Schlenker. Magnetism. Springer 2003.
- Segui, C.; Pons, J. & Cesari, E. Effect of atomic ordering on the phase transformations in *Ni-Mn-Ga* shape memory alloys. *Acta Materialia*, 2007, **55**, 1649.
- Chernenko, V.A.; Pons, J.; Segui, C. & Cesari, E. *Acta Materialia*, 2003, **50**, 53.
- Murray, S.J.; Farinelli, M.; Kantner, C.; Huang, J.K.; Allen, S.M. & O'Handley, R.C. *J. Appl. Phys.*, 1988, **83**, 72-97.
- Kudrvtsev, Y.V.; Lee, Y.P. & Rhea, J.Y. Structural and temperature dependence of the optical and magneto-optical properties of the Heusler *Ni₂MnGa* alloy. *Physics Review B*, 2002, **66**, 115-14.

Contributors



Dr R.P. Mathur obtained BE from Rajasthan University, Jaipur, and MTech from Indian Institute of Technology, Kanpur, in 1982 and 1991, respectively. He has obtained his PhD from Indian Institute of Technology, Roorkee, in 2008. Presently, he is working as a Scientist at Defence Metallurgical Research Laboratory (DMRL), Hyderabad. His areas

of research interest include: amorphous alloys, nanostructured soft/hard magnetic materials, rare earth permanent magnets, functional materials such as shape memory alloys. He has published about 25 research papers in reputed international journals and more than 30 papers in national/ international conference proceedings.



Mr R.K. Singh obtained his BTech (Metallurgical Engineering) from the Indian Institute of Technology, Roorkee, and MTech (Metallurgy) from Institute of Technology, Banaras Hindu University, Varanasi, in 2002 and 2006, respectively. Presently, he is working as Scientist at DMRL, Hyderabad. His research area includes: development of ferromagnetic shape memory alloys, *Ni-Ti* based shape

memory alloys, *Sm-Co*-based permanent magnets and other magnetic materials for defence applications.



Prof (Dr) Subrata Ray obtained his MTech and PhD from IIT, Kanpur. Presently, he is working as Professor, Metallurgical and Materials Engineering in University of Roorkee. He has research interests in materials development with special emphasis on cast metal matrix composites (MMC). He has many pioneering contribution in cast MMC including introduction of stir-casting and

addition of surface active elements for which he held the first patent. He has also developed interest on materials used in *Li-ion* batteries. He has published more than 200 technical papers, mostly in international journals and handbooks including those of ASM and ASLE. He is a fellow of the National Academy of Sciences, India, and Indian National Academy of Engineering.



Dr M. Manivel Raja obtained BSc and MSc(Physics) from the Madurai-Kamaraj University, Madurai, in 1989 and 1991, respectively, and PhD (Nuclear Physics) from the University of Madras, Chennai, in 1997. Presently, he is working as a Scientist at DMRL, Hyderabad. After graduating, he spent five years as post-doctoral fellow at University of New

York, Stony Brook and was involved in research and development of magnetic thin film sensors and devices. He is conducting research on magnetism and magnetic materials. He has published 45 research papers in reputed international journals and more than 60 papers in national/ international conference proceedings.



Dr Partha Ghosal obtained PhD in Metallurgical Engineering from IT, Banaras Hindu University in 1996. Presently, he is working as a Scientist in the Electron Microscopy Group at DMRL. He is recipient of *Young Microscopists Award* (2001) from EMSI and *DRDO-Laboratory Scientist of the Year Award* (2006). His research interests are nanomaterials

characterisation and defects characterisation using electron microscopy and has more than 15 years of experience. He has published 35 research papers in reputed international journals and more than 45 papers in national/international conference proceedings/presentations. He has delivered 25 invited lectures and is the author of 2 patents. He is a life member of IIM, EMSI, MSI and MRSI.



Dr V. Chandrasekaran obtained his PhD from Annamali University, Tamil Nadu. He is Ex-senior scientist of DMRL. His areas of research interest include: Rare earth permanent magnets, magnetostrictive, magnetocaloric, ferromagnetic shape memory and nanostructured soft/hard materials. He has published more than 40 papers in international journals. He was a recipient of *MRSI medal* (1990),

Vasvik Industrial Research Award (1991) and *Metallurgist of the Year Award* (1998).